Supporting Information

A Synergistic Approach Combining Cu Doping and CuO/C Intertwined Network for the $Na_4Fe_3(PO_4)_2P_2O_7$ Cathode: Enhancing High-Rate Performance and Structural Robustness

Yuhan Huang [a], Jie Liao [a], Wendou Pei [a], Yaohan Fei [a], Wei Li [a], Jinli Zhang [a]*

[a] School of Chemical Engineering and Technology, Tianjin University, Tianjin, 300072, P. R. China

*Corresponding Author: E-mail: zhangjinli@tju.edu.cn

Contents

6) **Table S6** Electrochemical performance of HC anodes pre-sodiated with varying contact durations.

7) **Table S7** Comparison for electrochemical performance of NFPP-Cu4||HC full cell with other reported NFPP-based full-cell devices.

1. Experimental

1.1 Materials Synthesis

All chemical reagents were commercially available analytical grade products, purchased from commercial sources and used without further purification. The ferrous phosphate precursor ($Fe_3(PO_4)_2$) for NFPP was synthesized via a liquid-phase precipitation method. Specifically, an aqueous solution containing 0.6 M ferrous sulfate ($FeSO_4·7H_2O$, 99.5%, Kemiou) and 0.12 M ascorbic acid ($C_6H_8O_6$, 99.0%, Kemiou) was first prepared. Subsequently, a 0.4 M sodium phosphate solution (Na_3PO_4, 99.8%, Aladdin) was slowly pumped into the mixture. The reaction system was continuously stirred at 70 °C with a stirring speed of 300 rpm for 120 min. The resulting precipitate was collected by filtration, dried, and then calcined to obtain the $Fe_3(PO_4)_2$ precursor. The as-prepared $Fe_3(PO_4)_2$ was mixed with sodium acetate ($NaCH_3COO$, 99.0%, Aladdin) and ammonium dihydrogen phosphate ($NH_4H_2PO_4$, 99.0%, Aladdin) in stoichiometric ratios. Using glucose ($C_6H_{12}O_6$, 99.5%, Aladdin) as a carbon source, the mixture was ball-milled for 3.5 h and then subjected to a two-step calcination under an argon atmosphere: first at 300 °C for 6 h, followed by 550 °C for 12 h, to obtain the final NFPP product. Finally, the as-synthesized NFPP material was mixed with copper nitrate ($Cu(NO_3)_2·3H_2O$, 98.0%, Aladdin) at a mass ratio of 1:x (x = 0.02, 0.04, and 0.06). The mixture was ground in anhydrous ethanol for 20 min and then calcined at 300 °C for 3 h to yield the corresponding Cu-modified NFPP samples. For the sake of simplified discussion, the modified samples were designated as NFPP-Cu2, NFPP-Cu4, and NFPP-Cu6, with the corresponding x values of 0.02, 0.04, and 0.06.

1.2 Physical Characterizations

The crystal structures of the materials were analyzed using an X-ray diffractometer (XRD, Rigaku, SmartLab) with a Cu-Kα radiation source at a scanning rate of 1° min^{-1}. The acquired X-ray diffraction patterns were further analyzed via GSAS-II software to obtain more comprehensive crystal structure data. The surface morphology of the materials was observed using a field-emission scanning electron microscope (SEM, FEI

Apreo S LoVac). The internal structure of the materials was characterized by a high-resolution transmission electron microscopy (HR-TEM, JEOL JEM-F200) to acquire high-resolution images, which was supplemented by energy-dispersive X-ray spectroscopy (EDS) elemental mapping. The elemental composition and chemical states on the surface of the materials were analyzed via X-ray photoelectron spectroscopy (XPS, Thermo Fisher Science K-Alpha^{+}). The acquired XPS data were fitted using Avantage software, with the C—C bond at 284.8 eV in the C 1s spectrum employed as the reference for charge correction. Fourier transform infrared (FT-IR, Bruker INVENIO) spectroscopy was employed to identify the vibrational modes of functional groups within the wavenumber range of 400–1400 cm^{-1}. Raman spectra were acquired using a Raman spectrometer (Renishaw). The intensity ratios of the D to G bands, obtained by peak deconvolution (Origin software), were used to evaluate the graphitization degree of the carbon. The band gaps of the materials were analyzed by in situ ultraviolet-visible-near-infrared (UV-Vis-NIR) spectroscopy (PE Lambda 1050). The carbon content was quantitatively determined by thermogravimetric analysis (TGA, Mettler Toledo TGA/DSC 2).

1.3 Electrochemical Measurements

The electrochemical properties of the materials were evaluated using CR-2032 type coin half and full cells. All electrochemical measurements were performed at room temperature (25 °C). For the cathode electrode, the active material, polyvinylidene fluoride (PVDF) binder, and conductive agent (Super P) were mixed quantitatively at a mass ratio of 8:1:1. An appropriate amount of N-methyl-2-pyrrolidone (NMP) was added, and the mixture was thoroughly stirred before being coated onto aluminum foil. The coated foil was then dried in an oven at 120 °C for 10 h, with the average loading of the active material being 1.5–1.8 mg cm^{-2}. The half-cells were assembled using metallic sodium foils as the counter electrodes, glass fiber (Whatman, GF/D) as the separators, and the electrolyte prepared by dissolving 1 M sodium perchlorate ($NaClO_4$) in a mixed solvent of propylene carbonate (PC) with 5% fluoroethylene carbonate (FEC) as the additive. After assembly, the cells were aged for at least 6 hours prior to

testing. Galvanostatic charge-discharge (GCD) and galvanostatic intermittent titration technique (GITT) tests were conducted on a Land CT3001A test system. The GITT measurements were performed at a current density of 0.1 C with a pulse time of 20 minutes, followed by a relaxation period of 60 minutes. Cyclic voltammetry (CV) and electrochemical impedance spectroscopy (EIS) measurements were carried out on a CORRTEST CS310X electrochemical workstation. CV measurements were conducted in the voltage range of 1.5–4.0 V at various scan rates from 0.1 to 1.0 mV s^{-1}. EIS measurements were performed over a frequency range of 0.01 to 1×10^5 Hz with a voltage amplitude of 5 mV. For the full cells, the hard carbon (HC) anode was fabricated following a procedure analogous to that of the cathode. Prior to full-cell assembly, the anode was pre-sodiated by contact with a metallic sodium foil for 12 hours to form a stable solid electrolyte interphase (SEI) layer, and then paired with the NFPP-based cathode to assemble the full cells. Galvanostatic charge-discharge measurements of the full cells were performed within a voltage window of 1.5–4.0 V (vs. Na^+/Na).

2. Supplementary Figures

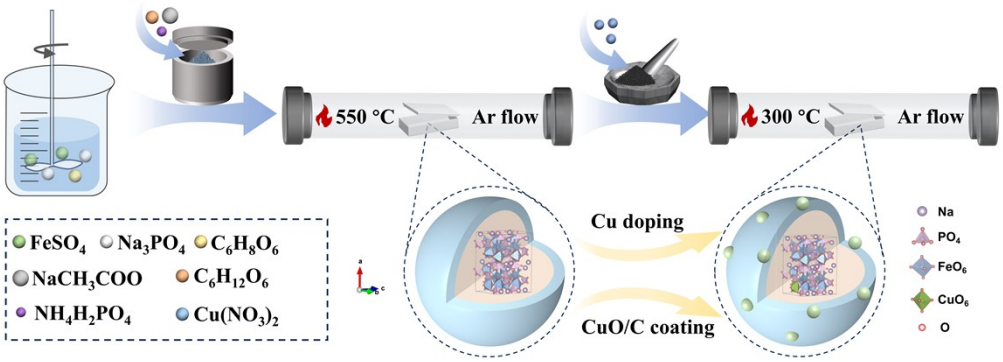

Fig. S1 Schematic diagram of the synthesis process.

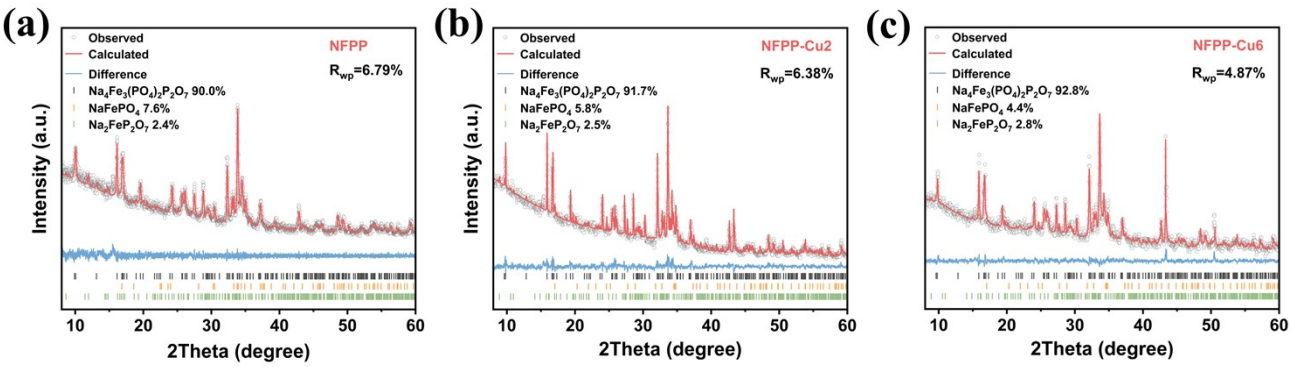

Fig. S2 XRD Rietveld refinement patterns of (a) NFPP, (b) NFPP-Cu2 and (c) NFPP-Cu6.

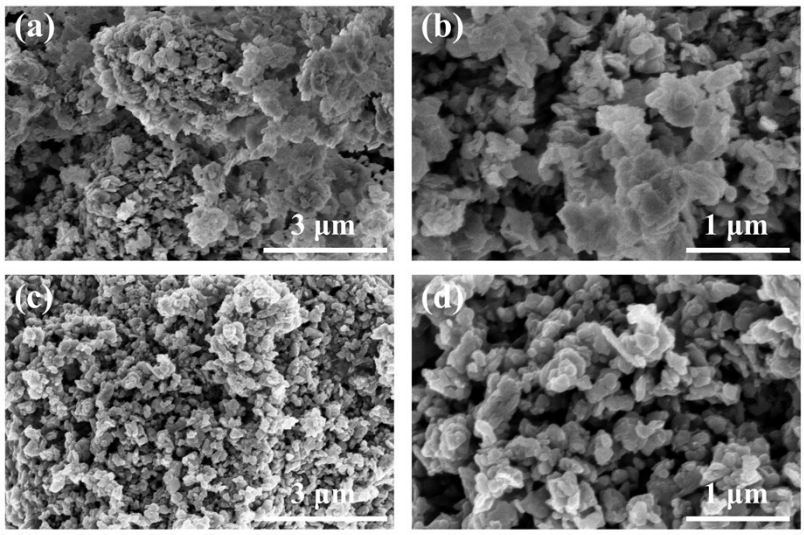

Fig. S3 SEM images of NFPP and NFPP-Cu4.

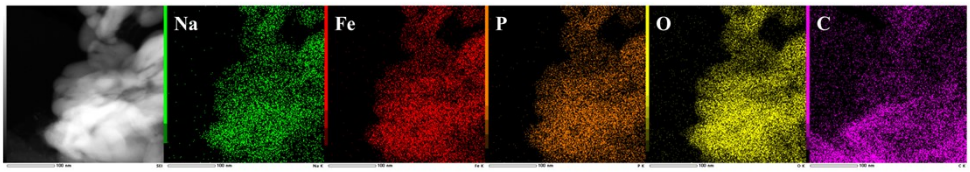

Fig. S4 EDS elemental mapping images of NFPP.

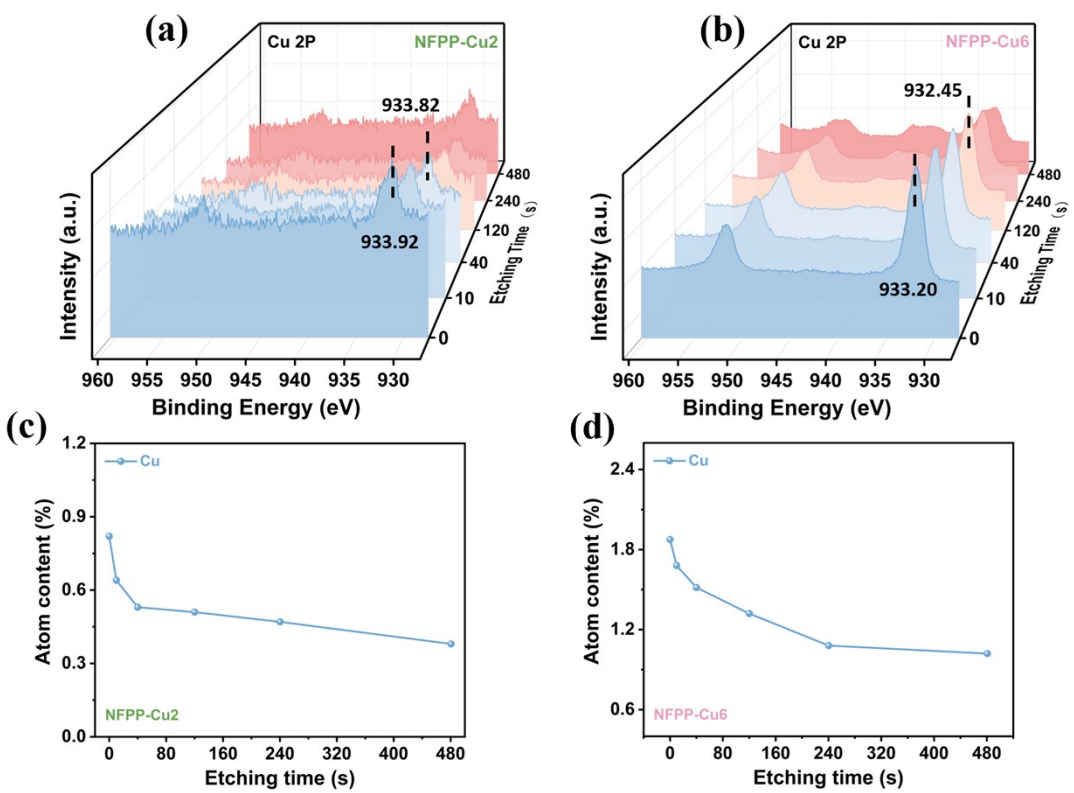

Fig. S5 Cu 2p XPS spectra of (a) NFPP-Cu2 and (b) NFPP-Cu6 within the etching time of 0–480 s. Relative contents of Cu elements inside (c) NFPP-Cu2 and (d) NFPP-Cu6 versus the etching time.

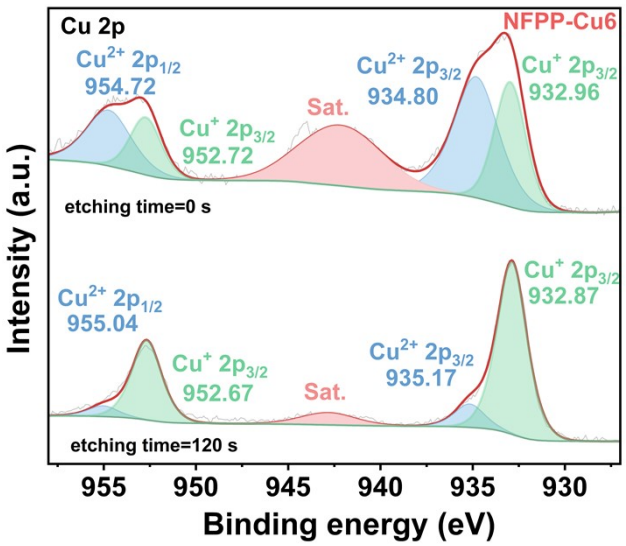

Fig. S6 Deconvoluted Cu 2p XPS spectra of NFPP-Cu6.

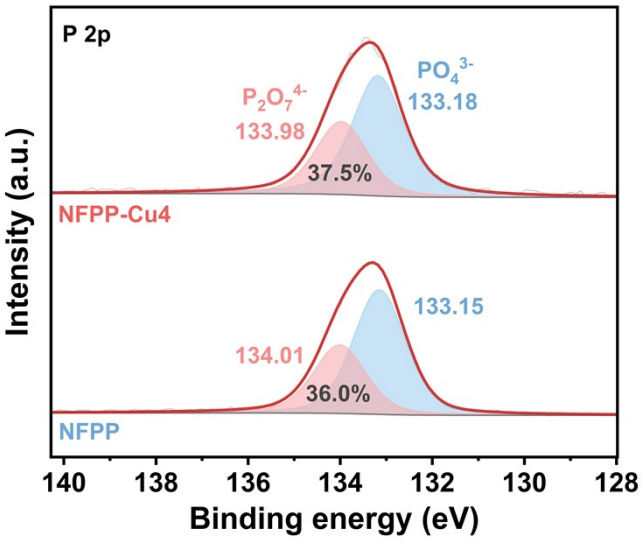

Fig. S7 High-resolution XPS spectra for P 2p in NFPP.

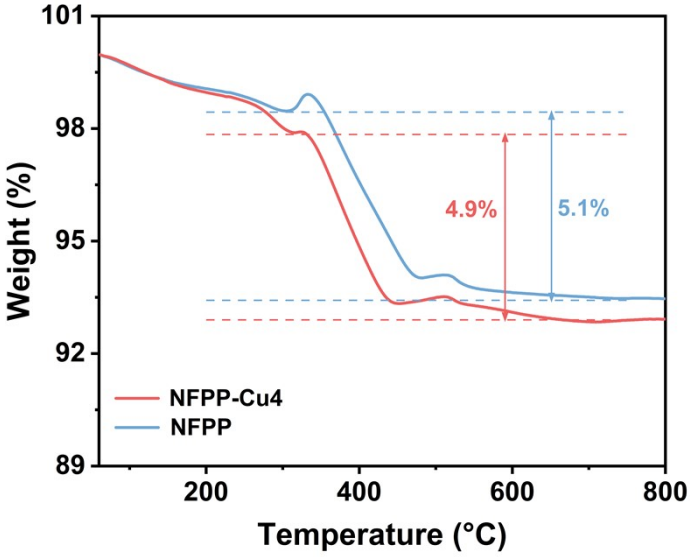

Fig. S8 TGA curves of NFPP and NFPP-Cu4.

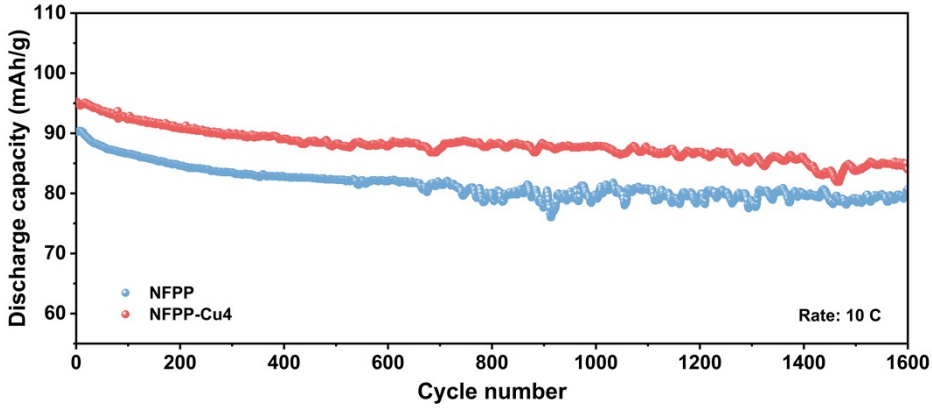

Fig. S9 Long cycling performance of NFPP and NFPP-Cu4 at 10 C.

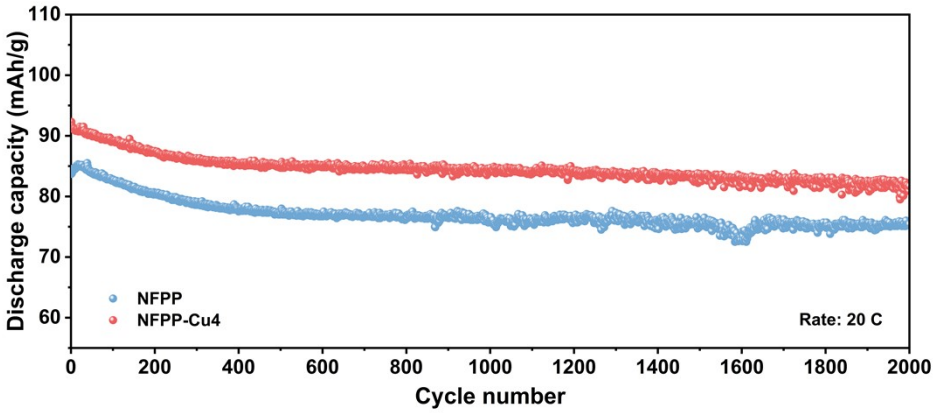

Fig. S10 Long cycling performance of NFPP and NFPP-Cu4 at 20 C.

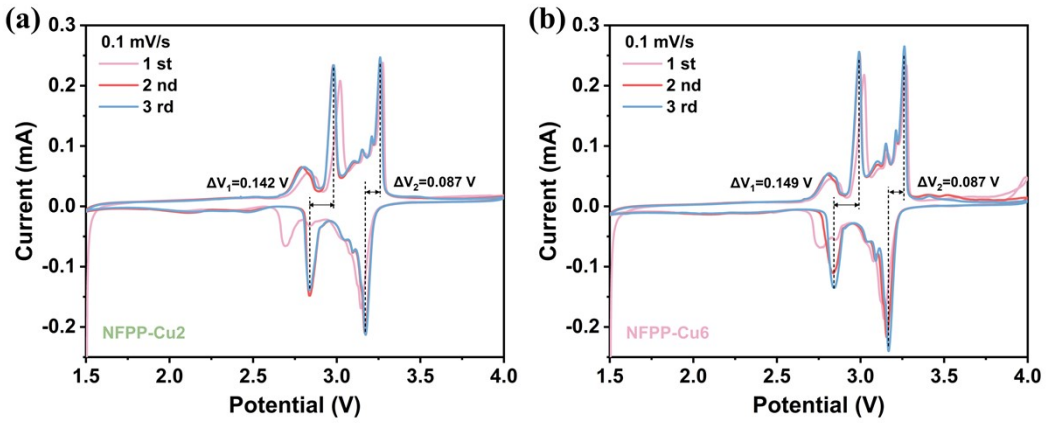

Fig. S11 CV curves of (a) NFPP-Cu2 and (b) NFPP-Cu6 for the first three cycles at 0.1 mV s^{-1}.

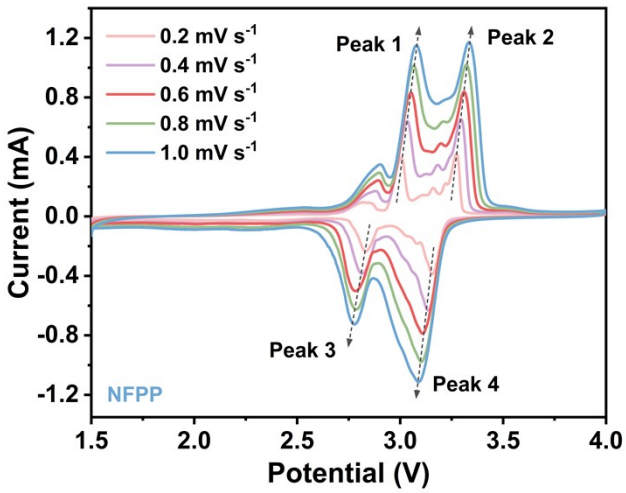

Fig. S12 CV curves of NFPP at gradient scan rates from 0.2 to 1.0 mV s^{-1}.

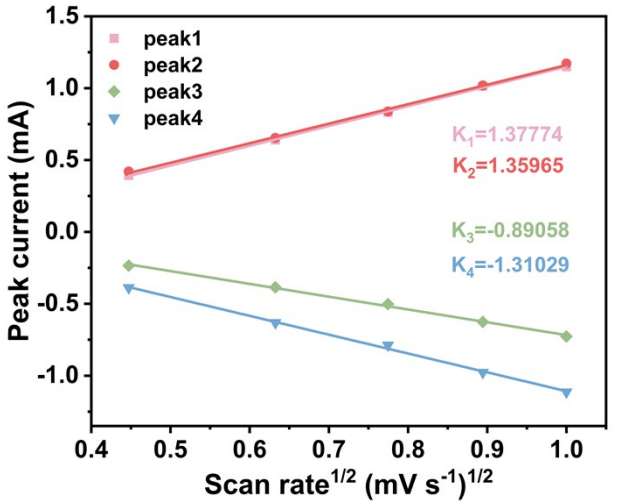

Fig. S13 Linear fit between the peak current and the square root of the scan rate.

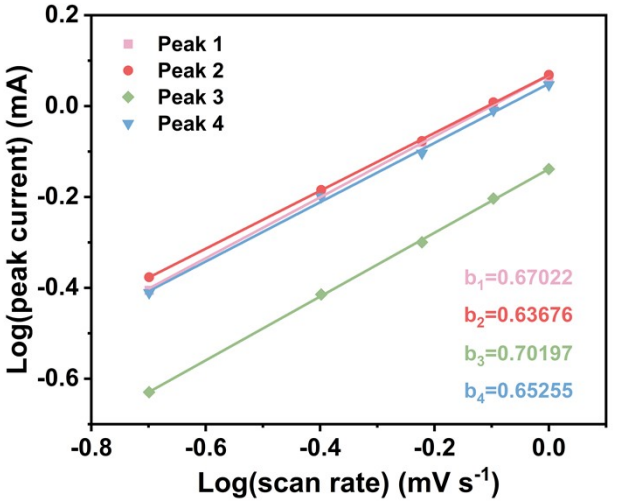

Fig. S14 Calculated b-values of different redox peaks.

To further investigate the kinetic characteristics of NFPP and NFPP-Cu4, CV measurements were conducted at varying scan rates from 0.2 to 1.0 mV s^{-1} within a voltage window of 1.5–4.0 V. Based on the relationship between the redox peak current and the square root of the scan rate, the sodium-ion diffusion coefficient (D_{Na^+}) can be quantified using the Randles-Sevcik equation:[1]

$$i_p = 2.69 \times 10^5 n^{3/2} A D^{1/2} C_0 v^{1/2} \tag{1}$$

$$K = \frac{i_p}{v^{1/2}} \tag{2}$$

Herein, i_p is the peak current (A), n represents the number of electrons transferred per species in the reaction (n = 3 for this system), A denotes the electrode-electrolyte contact area (cm^2), D corresponds to the diffusion coefficient of sodium ions (Na^+) ($cm^2\ s^{-1}$), C_0 is the bulk concentration of sodium ions in the lattice (mol cm^{-3}), and v refers to the scan rate (mV s^{-1}).

Charge storage in the electrochemical process consists of two parts: a diffusion-controlled process and a pseudocapacitive process. To further elucidate the reaction kinetics of Na^+ storage in the structure of NFPP composites, the following equation is employed:[2]

$$i_p = a v^b \tag{3}$$

$$\log(i_p) = b \times \log(v) + \log a \tag{4}$$

Herein, i_p and v are the key variables, with a and b being the adjustable fitting coefficients. The b-value is used to distinguish the dominant kinetic process of the electrode: a value close to 1.0 indicates that the electrochemical reaction of the system is dominated by surface capacitive behavior, while a value close to 0.5 implies that the Faradaic process involving Na^+ insertion and extraction is diffusion-limited.[3]

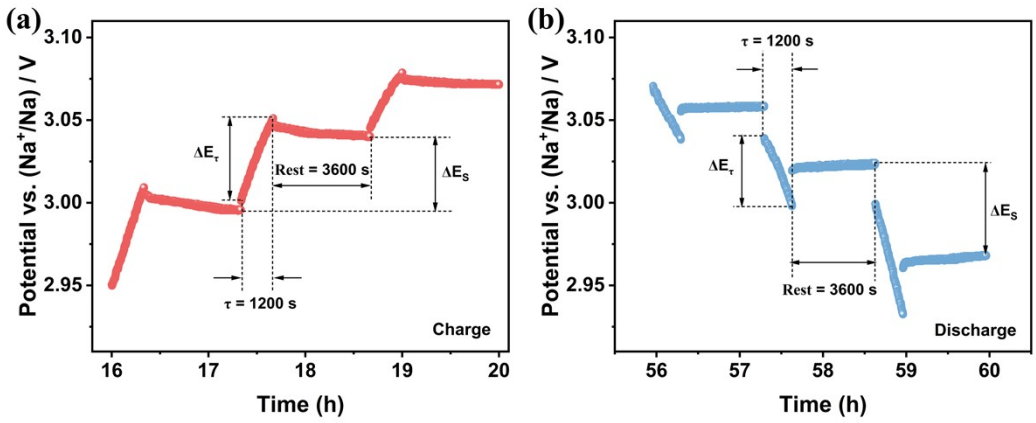

Fig. S15 Schematic illustration of selected steps in the GITT profile during charging and discharging for NFPP and NFPP-Cu4 electrode.

The sodium-ion diffusion coefficient (D_{Na^+}) was determined via GITT measurements. To ensure the complete formation of the cathode-electrolyte interphase (CEI), all coin cells were subjected to three initial cycles at 0.1 C (1 C = 129 mA g^{-1}) prior to GITT tests. The cells were then charged and discharged at the same current rate for 20 min, followed by a 60 min relaxation to attain a steady state for the system. This procedure was repeated across the voltage range of 1.5–4.0 V until completion. The sodium-ion diffusion coefficient D_{Na^+} can be calculated using the following equation:[4]

$$D_{Na+} = \frac{4}{\pi\tau}\left(\frac{m_B V_B}{M_B S}\right)^2\left(\frac{\Delta E_S}{\Delta E_\tau}\right)^2 \qquad \left(\tau \ll \frac{L^2}{D_{Na+}}\right) \tag{5}$$

Herein, D_{Na^+} denotes the sodium-ion diffusion coefficient (cm^2 s^{-1}), m_B is the mass loading of the electrode material (g), V_B represents the molar volume of the electrode material (cm^3 mol^{-1}), M_B corresponds to the molar mass of the material (g mol^{-1}), S refers to the electrode-electrolyte contact area (cm^2), τ is the constant current pulse time, ΔE_S is the potential difference between two consecutive steady-state voltages after the relaxation period, ΔE_τ is the total potential change of the cell during the constant current pulse, and L denotes the electrode thickness.

3. Supplementary Tables

Table S1 Detailed structural information of NFPP from Rietveld refinement.

Space Group: *Pn2$_1$a*		**Crystal system: Orthorhombic**			***α* = *β* = *γ* = 90°**
a = 18.00416 Å		**b = 6.54031 Å**	**c = 10.6720 Å**		**Volume = 1256.658 Å^3**
R_{wp} = 6.79%					**R_p = 3.18%**
Atom	***x***	***y***	***z***	***Occ.***	***Mult.***
Fe1	0.14301	0.96952	0.12277	1	4
Fe2	0.13703	0.52152	0.11112	1	4
Fe3	0.26834	0.26353	0.85494	1	4
P1	0.09646	0.79920	0.07806	1	4
P2	0.08628	0.24812	1.03459	1	4
P3	0.18664	0.49469	0.57997	1	4
P4	0.19955	1.03715	0.62518	1	4
Na1	-0.08413	0.55304	0.83149	1	4
Na2	-0.00706	0.93557	0.75007	1	4
Na3	0.10831	0.25181	0.30997	1	4
Na4	0.27044	0.71318	0.85622	1	4
O1	0.05930	0.68829	0.01677	1	4
O2	0.00623	0.75457	0.43619	1	4
O3	0.17070	0.54664	-0.05410	1	4
O4	0.05442	0.35364	0.09898	1	4
O5	0.05132	0.17479	-0.05219	1	4
O6	0.10967	0.27372	0.75775	1	4
O7	0.14927	0.50573	0.58576	1	4
O8	0.02349	0.81086	0.11928	1	4
O9	0.02091	0.48781	0.77522	1	4
O10	0.16651	0.07010	0.39508	1	4
O11	0.17889	0.95708	0.74836	1	4
O12	0.13815	0.50330	0.75749	1	4
O13	0.31815	0.57078	0.58111	1	4
O14	0.24718	0.43387	0.01710	1	4
O15	0.26982	0.66874	0.24957	1	4

Table S2 Detailed structural information of NFPP-Cu4 from Rietveld refinement.

Space Group: *Pn2$_1$a*	**Crystal system: Orthorhombic**		**$\alpha = \beta = \gamma = 90°$**	
a = 17.99988 Å	**b = 6.52545 Å**	**c = 10.64270 Å**	**Volume = 1250.062 Å^3**	
R_{wp} = 4.05%			**R_p = 5.34%**	
Atom	***x***	***y***	***z***	***Occ.***	***Mult.***
Fe1	0.17379	1.02164	0.17571	1	4
Fe2	0.14410	0.49714	0.17922	0.95	4
Fe3	0.24332	0.28250	0.81350	1	4
P1	0.05413	0.72328	0.14435	1	4
P2	0.03772	0.21747	0.98187	1	4
P3	0.19289	0.57465	0.62177	1	4
P4	0.22277	1.00950	0.69972	1	4
Na1	0.00017	0.49150	0.85381	1	4
Na2	0.03815	0.90011	0.62326	1	4
Na3	0.07534	0.20178	0.35716	1	4
Na4	0.28639	0.80298	0.67726	1	4
O1	-0.01729	0.88991	0.00023	1	4
O2	-0.00668	0.76908	0.33795	1	4
O3	0.03044	0.55176	0.08863	1	4
O4	0.03367	0.36111	0.12867	1	4
O5	0.07771	0.19761	0.09936	1	4
O6	0.15358	0.23848	0.73058	1	4
O7	0.14442	0.46975	0.47241	1	4
O8	0.12887	0.75300	0.17847	1	4
O9	0.19501	0.53211	0.77412	1	4
O10	0.14821	0.00519	0.50801	1	4
O11	0.17435	0.98645	0.91320	1	4
O12	0.29695	0.32038	0.64563	1	4
O13	0.22283	0.64389	0.62044	1	4
O14	0.23526	0.37113	0.15875	1	4
O15	0.26237	0.69308	0.11403	1	4
Cu	0.10768	0.92586	0.25897	0.05	4

Table S3 XPS C 1s peak deconvolution data of NFPP and NFPP-Cu4.

Sample	NFPP		NFPP-Cu4	
	Peak BE (eV)	Area ratio	Peak BE (eV)	Area ratio
sp^2 C	284.76	60.65%	284.79	69.28%
sp^3 C	285.98	21.81%	286.30	14.69%
C–O	287.55	7.85%	287.85	7.39%
O–C=C	289.27	9.69%	289.33	8.64%

In X-ray photoelectron spectroscopy (XPS) analysis, the proportion of sp^2-hybridized carbon in carbon-based materials is determined by peak deconvolution of the C 1s spectrum. After peak fitting, the percentage of sp^2-hybridized carbon is calculated by dividing the area of the sp^2 peak by the total area of all C 1s peaks.

$$sp^2\% = \left(\frac{Area\ of\ sp^2\ peak}{Total\ area\ of\ C\ 1s\ peaks}\right) \times 100\% \quad (6)$$

The relative concentrations of all other Spectral components were determined using the same quantification method.

Table S4 XPS Fe 2p peak deconvolution data of NFPP and NFPP-Cu4.

Sample	NFPP		NFPP-Cu4	
	Peak BE (eV)	Area ratio%	Peak BE (eV)	Area ratio%
Fe^{2+}2p3/2	710.61	68.23%	710.72	70.13%
Fe^{2+}2p1/2	724.08		724.10	
Fe^{3+}2p3/2	713.39	31.77%	713.87	29.87%
Fe^{3+}2p1/2	726.91		727.09	

Table S5 EIS fitting results.

Sample	R_{ct} (ohms)	
	1st	100th
NFPP	212.0	263.3
NFPP-Cu4	158.8	174.4

Table S6 Electrochemical performance of HC anodes pre-sodiated with varying contact durations.

Pre-sodiation time (h)	Initial Coulombic efficiency (%)	Cycling stability	State
2	78.56	Poor	Under-sodiated
4	85.22	Poor	Under-sodiated
8	92.35	Moderate	Near-optimal
12	97.81	Excellent	Optimal
16	96.61	Decreased	Over-sodiated

The commercial HC anode was contacted with metallic sodium foil in an argon-filled glovebox with a controlled amount of electrolyte. The contact time was systematically varied from 2 h to 16 h, and the resulting electrochemical performance was evaluated.

The 12 h condition delivers the highest initial Coulombic efficiency (97.81%) and excellent cycling stability, representing the optimal balance between sufficient SEI formation and avoidance of over-sodiation. Shorter durations (2–8 h) yield incomplete SEI formation with lower ICE, while prolonged contact (16 h) causes SEI overgrowth and compromised cycling performance despite comparable initial ICE.

The uniform SEI formation is achieved through controlled interfacial reaction kinetics between the Na foil and hard carbon. By directly contacting the sodium metal with the electrode, sodium ions and electrons migrate easily due to the potential difference between the sodium metal and the electrode material, enabling homogeneous Na+ distribution across the electrode surface. The moderate pre-sodiation degree at 12 h ensures a thin and uniform pre-SEI passivation layer, which prevents excessive

electrolyte decomposition and facilitates the formation of a dense, stable SEI film during subsequent cycling. This time-dependent behavior demonstrates that the SEI formation process is inherently self-regulating when contact time is precisely controlled.

Table S7 Comparison for electrochemical performance of NFPP-Cu4||HC full cell with other reported NFPP-based full-cell devices.

Sample	Voltage (V)	Initial capacity (mA h g^{-1}), rate	Cycle performance	Ref.
NFPPHE||HC	1.5–4.3	80.4, 0.5 C 37.4, 5 C	76.0%, (300^{th}, 0.5 C)	[5]
NFPP-0.3Cu||HC	1.5–4.2	108.0, 1 C 55.8, 5 C	82.0%, (100^{th}, 1 C)	[6]
NKFPP||HC	2.0–4.0	86.5, 5 C	76.6%, (500^{th}, 5 C)	[7]
NMFPPNb-2||HC	1.7–4.3	81.7, 1 C 62.8, 5 C	87.2%, (150^{th}, 1 C)	[8]
HEV-HFPP||HC	1.75–4.25	82.8, 10 C	62.0%, (700^{th}, 0.5 A g^{-1})	[9]
NFPP-Cu4||HC	1.5–4.0	102.7, 0.2 C 89.5, 5 C	92.7%, (500^{th}, 5 C)	This work

References

[1] X. Bao, Y. Wang, G. Chen, N. Qin, X. Wang, Y. He, Y. Shen, L. Chen, Y. Zhang, G. Cui and Z.-F. Ma, *Adv. Funct. Mater.*, 2025, **35**, 2506242.

[2] J. Gao, H. Chen, Y. Mei, L. Ni, H. Wang, J. Huang, N. Hong, B. Song, Y. Tian, W. Deng and G. Zou, *Nano Energy*, 2023, **115**, 108747.

[3] Q. Xia, L. Zhang, D. Wang, J. Wang, Z. Xu, Y. Zhang, Z. Yao, Y. Guo, P. Jia, L. Zhang and Y. Yang, *Energy Storage Mater.*, 2025, **84**, 104849.

[4] P. Dong, F. Peng, Q. Zhang, H. Wang, Y. Chu, C. Chen and C. Yang, *Angew. Chem., Int. Ed.*, 2025, **64**, e202502693.

[5] Y. Qiu, Q. Shi, X. Yu, Y. Liu, Y. Liu, W. Feng, J. Wang and Y. Zhao, *Chem. Eng. Sci.*, 2024, **300**, 120671.

[6] X. Qi, Q. Dong, H. Dong, B. Hou, H. Liu, N. Shang, S. Zhang, L. Wang, H. Shao, Y. Shen and S. Chen, *Energy Storage Mater.*, 2024, **73**, 103861.

[7] S. Wang, Q. Zhang, H. Zhu, Y. Du, K. Yu, D. Zhou, Y. Deng, J. Wang and J. Jian, *Adv. Funct. Mater.*, 2025, DOI: 10.1002/adfm.202520871.

[8] J. Zeng, J. Gao, W. Jian, H. Wang, W. Li, N. Hong, B. Zhang, J. Huang, B. Song, C. Gan and S. Yasar, *Adv. Funct. Mater.*, 2024, **34**, 2410992.

[9] X. Hu, S. Liang, J. Lin, W. Ren, S. Fu, Z. Cao, T. Zhang, L. Zhang and X. Cao, *Adv. Energy Mater.*, 2025, **15**, 2404965.